

 Open access • Journal Article • DOI:10.1007/S11119-015-9390-0

Sequential application of hyperspectral indices for delineation of stripe rust infection and nitrogen deficiency in wheat — [Source link](#)

[Rakshesh Devadas](#), [Rakshesh Devadas](#), [David Lamb](#), [David Lamb](#) ...+2 more authors

Institutions: [University of Technology, Sydney](#), [Cooperative Research Centre](#), [University of New England \(Australia\)](#)

Published on: 22 Mar 2015 - [Precision Agriculture](#) (Springer US)

Topics: [Rust](#)

Related papers:

- [Development of spectral indices for detecting and identifying plant diseases](#)
- [Detecting sugarcane 'orange rust' disease using EO-1 Hyperion hyperspectral imagery](#)
- [Plant Disease Detection by Imaging Sensors - Parallels and Specific Demands for Precision Agriculture and Plant Phenotyping.](#)
- [Evaluating ten spectral vegetation indices for identifying rust infection in individual wheat leaves](#)
- [Detection of soybean rust using a multispectral image sensor](#)

Share this paper:    

View more about this paper here: <https://typeset.io/papers/sequential-application-of-hyperspectral-indices-for-4y1hdddlj6>

Sequential application of hyperspectral indices for delineation of stripe rust infection and nitrogen deficiency in wheat

R. Devadas^{a,b*}, D. W. Lamb^{bc}, D. Backhouse^d & S. Simpfendorfer^e

^aClimate Change Cluster (C3), Faculty of Sciences, University of Technology Sydney, PO Box 123, Broadway, NSW 2007, Australia

Phone: +61 2 9514 8351, Email: rakshesh.devadas@uts.edu.au

^bCooperative Research Centre for Spatial Information, P.O. Box 672 Carlton South, VIC, Australia 3053

^cPrecision Agriculture Research Group, University of New England, Armidale, NSW 2351, Australia

dlamb@une.edu.au

^dSchool of Environmental and Rural Science, University of New England, Armidale, NSW 2351, Australia

dbackhou@une.edu.au

^eNSW Department of Primary Industries, Tamworth, NSW 2340, Australia

steven.simpfendorfer@dpi.nsw.gov.au

* Corresponding author

Abstract

Nitrogen (N) fertilization is crucial for the growth and development of wheat crops, and yet increased use of N can also result in increased stripe rust severity. Stripe rust infection and N deficiency both cause changes in foliar physiological activity and reduction in plant pigments that result in chlorosis. Furthermore, stripe rust produce pustules on the leaf surface which similar to chlorotic regions have a yellow color. Quantifying the severity of each factor is critical for adopting appropriate management practices. Eleven widely-used vegetation indices (VIs), based on mathematic combinations of narrow-band optical reflectance measurements in the visible/near infrared wavelength range were evaluated for their ability to discriminate and quantify stripe rust severity and N deficiency in a rust-susceptible wheat variety (H45) under varying conditions of nitrogen status. The Physiological Reflectance Index (PhRI) and Leaf and Canopy Chlorophyll Index (LCCI) provided the strongest correlation with levels of rust infection and N-deficiency, respectively. When PhRI and LCCI were used in a sequence, both N deficiency and rust infection levels were correctly classified in 82.5% and 55% of the plots at Zadoks growth stage 47 and 75,

1
2
3
4
5
6
7
8
9
10
11
12
13
14
15
16
17
18
19
20
21
22
23
24
25
26
27
28
29
30
31
32
33
34
35
36
37
38
39
40
41
42
43
44
45
46
47
48
49
50
51
52
53
54
55
56
57
58
59
60
61
62
63
64
65

respectively. In misclassified plots, an overestimation of N deficiency was accompanied by an underestimation of the rust infection level or vice-versa. In 18% of the plots, there was a tendency to underestimate the severity of stripe rust infection even though the N-deficiency level was correctly predicted. The contrasting responses of the PhRI and LCCI to stripe rust infection and N deficiency, respectively, and the relative insensitivity of these indices to the other parameter makes their use in combination suitable for quantifying levels of stripe rust infection and N deficiency in wheat crops under field conditions.

Key words: Wheat rust, nitrogen, vegetation index, remote sensing, hyperspectral

Introduction

1 Nitrogen (N) nutrition is considered an important factor affecting the quantitative resistance of
2 wheat to rust diseases and high N is associated with increased severity of rust infection. Several
3 studies (Bryson et al. 1997; Jensen and Munk 1997) have identified a range of mechanisms
4 associated with this response including (i) changes in biochemical processes in the plant, such as
5 decreased phenol content and (ii) changes to the crop canopy structure creating a more favorable
6 microclimate for rust infection as a result of increased crop density and canopy size.
7
8
9

10 N is the most important fertilizer element determining the productivity of crops (Caviglia and
11 Sadras 2001; Muurinen and Peltonen-Sainio 2006). Increased N supply results in increased
12 chlorophyll content and leaf greenness, particularly of the older leaves. This will also lead to an
13 increase in leaf size, tiller production and height, delay in leaf senescence, and boost grain
14 formation (Gooding and Davies 1997).
15
16

17 Infection by rust pathogens or manifestation of N deficiency both cause similar changes in foliar
18 color; the former through the appearance of yellow pustules and both resulting in chlorosis. Even
19 though both rust infection and N deficiency cause yellowing, management practises are entirely
20 different. Rust infection necessitates application of appropriate fungicides, while N deficiency
21 needs to be corrected by fertilizer application, and this in turn may exacerbate any concomitant rust
22 infection (Bryson et al. 1997; Jensen and Munk 1997) Thus, discrimination of N deficiency from
23 rust infection is critical for crop management aimed at achieving a yield target.
24
25
26

27 Developments in optical sensor technology and remote sensing techniques including ground
28 based sensors, aerial photography and satellite imaging systems, have created enormous potential to
29 measure vegetation characteristics non-destructively at varying spatial scales. Application of these
30 techniques is based on the spectral reflectance characteristics of the plant canopy which in turn is
31 dependent on the vegetative health, pigment and photochemical content of the leaf and canopy
32 morphology. Numerous simple and cost-effective optical devices can sense objects with a larger
33 spectral range than the human eye (Hatfield 1993; Moshou et al. 2005; Nicolas 2004; Qin and
34 Zhang 2005) which, based on the measurement of canopy reflectance in several wavebands, would
35
36
37
38
39
40
41
42
43
44
45
46
47
48
49
50
51
52
53
54
55
56
57
58
59
60
61
62
63
64
65

1
2
3
4
5
6
7
8
9
10
11
12
13
14
15
16
17
18
19
20
21
22
23
24
25
26
27
28
29
30
31
32
33
34
35
36
37
38
39
40
41
42
43
44
45
46
47
48
49
50
51
52
53
54
55
56
57
58
59
60
61
62
63
64
65

allow plant vigor and disease stress patches to be spatially identified and mapped. With more and more remote sensing data being available from various platforms, mapping vegetation stress across large areas can be carried out cost effectively without observer bias and error.

A hyperspectral imaging system, also known as an "imaging spectrometer", acquires images in a number of narrow, contiguous spectral bands. Use of narrow spectral bandwidth sensors can capture the subtle variations in the spectral reflectance characteristics of a ground cover (Aspinall et al. 2002; Gao 1999). Several studies have employed hyperspectral imaging techniques for monitoring crop stress due to various factors including disease infection and N deficiency. Spectral reflectance for wavebands of 680 ± 10 , 725 ± 10 and 750 ± 10 nm were proven to be very effective for the discrimination of stripe rust infected plants from healthy plants (Moshou et al. 2005; Bravo et al. 2003). The potential of the photochemical reflectance index (PRI) for quantifying stripe rust levels using proximal and aerial hyperspectral imagery was demonstrated by Huang et al. (2007).

In recent years, up to 50 vegetation indices (VIs) have been proposed and investigated for a range of targeted applications in crops including identifying, quantifying or discriminating water stress, disease, pests and nutritional status. A number of these are considered relevant to disease detection and nitrogen (N) nutrition in plants since physiological stress manifests itself in plants via changes to the balance of pigment composition, for example carotenoids, chlorophylls and xanthophylls (summarized in Table 1).

In our previous study (Devadas et al. 2009), ten widely-used VIs (Table 1) were evaluated for their ability to discriminate leaves of one month old wheat plants infected with yellow (stripe), leaf and stem rust. Narrow band indices like Anthocyanin Reflectance Index (ARI), representing changes in non-chlorophyll pigment concentration and the ratio of non-chlorophyll to chlorophyll pigments, proved more reliable in discriminating rust infected leaves from healthy plant tissue and is considered suitable for a disease presence/absence assessment.

The application of spectral data for the quantification of plant stress becomes complex in the context of an interaction effect of plant nutrition and disease manifestation. This is particularly relevant in the context of N-stripe rust interaction, where both N deficiency and rust incidence

1
2
3
4
5
6
7
8
9
10
11
12
13
14
15
16
17
18
19
20
21
22
23
24
25
26
27
28
29
30
31
32
33
34
35
36
37
38
39
40
41
42
43
44
45
46
47
48
49
50
51
52
53
54
55
56
57
58
59
60
61
62
63
64
65

results in chlorosis of the affected plants and becomes harder to detect at a broader scale. Paddock or regional level mapping of such stresses could be made possible with a thorough understanding of these interaction effects at field scale and identifying the appropriate spectral data and techniques to quantify them. In this context, this study assessed the potential of various hyperspectral indices to discriminate and quantify levels of N deficiency and stripe rust infection in field-grown wheat plants.

[Table 1 here]

Materials and methods

Field experiment and visual assessments

Field experimentation was conducted at the Breeza Research Station of the New South Wales Department of Primary Industries (NSW DPI) on the Liverpool Plains of northern NSW, Australia (150° 25' 31"E and 31° 10' 54"S). Wheat variety H45, a quick maturing variety with strong straw considered very susceptible to stripe rust (McRae et al. 2008), was grown during the period July to December 2007.

Plots were 10 m length and 1.8 m width. Spacing between rows was 40 cm and the sowing rate was adjusted to attain a target plant population of 100 plants/m². Nitrogen was added at sowing as urea at rates of 0, 50, 100, 200, and 300 kg N/ha. The whole trial was subjected to natural infection with wind-blown spores of the stripe rust fungus (*Puccinia striiformis*) from neighboring fields. Stripe rust was allowed to develop naturally in the '-fungicide' treatments by sowing untreated seed and applying no in-crop foliar fungicides to these plots. In contrast, to establish and maintain '+fungicide' treatments, the seed was treated prior to sowing with Jockey® (active ingredient 167 g/L fluquinconazole, Bayer Crop Science) at a rate of 450mL per 100 kg of seed. The '+fungicide' plots were also sprayed with the foliar fungicide Tilt® (active ingredient 250 g/L propiconazole, Syngenta) at a rate of 500mL/ha at flag leaf emergence (growth stage GS 39). This fungicide strategy ensured that the stripe rust severity in '+fungicide' plots was very low throughout the

growing season. There were four replicates of each treatment in a randomized complete block design.

Plots were rated for the severity of stripe rust infection at booting (GS 47) and during grain development (GS 75) on a standard scale used by the Australian Cereal Rust Laboratory, University of Sydney (Wellings and Bariana 2004). The scale measures the severity of stripe rust infection using scores ranging from 1 (no symptoms) to 9 (abundant sporulation across the whole leaf area). Scores for each plot were an average of responses for the two uppermost leaves of all plants in a plot at each assessment time.

A deficiency of nitrogen in wheat expresses first as yellowing of the lower leaves. As the deficiency increases with continuing crop growth, the chlorosis progresses to the upper leaves of the plant with yellowing generally occurring from the tip back towards the leaf base. Nitrogen deficiency was visually assessed on a scale ranging from 1 (no deficiency, green leaves through entire canopy) to 10 (highly deficient; lower canopy yellow and/or senescent and upper canopy yellow) based on ratings published by the International Maize and Wheat Improvement Centre (Snowball and Robson 1991).

Further, stripe rust infection and N deficiency observations were grouped into three classes each. A “Low” level rust infection class was formed by grouping plots with ACRL scores ranging from 1-3. Scores in the range of 4-6 and 7-9 were grouped into “Medium” and “High” classes, respectively. Similarly, plots were grouped into three levels of N deficiency: ‘Low’, ‘Medium’ and ‘High’, whose N deficiency scores ranged from 1-3, 4-7 and 8-10, respectively. The number of observations in each category is outlined in Table 2.

[Table 2 here]

Leaf chlorophyll content

A chlorophyll meter (SPAD 502, Spectrum Technologies, Inc., Plainfield, IL, USA) was used to determine the relative amount of chlorophyll in the leaves. These measurements (SPAD values) are made on the basis of light absorption characteristics of chlorophyll in the wavelength of 650 nm and 940 nm (Spectrum 2009). SPAD values recorded at growth stage GS 75 were compared with the

1 qualitative visual N deficiency scores (Fig 1) and thus enabled the comparison of qualitative and
2 quantitative measure of crop N status. As expected, high recorded SPAD values corresponded to
3 observed low N deficiency scores and vice versa. The relationship showed a non-linear trend as
4 SPAD values did not vary much with the change in the lower range of N deficiency scores.
5

6
7 [Fig 1 here]
8

9 ***Hyperspectral data collection***

10 Reflectance spectra were collected using a wavelength spectrometer consisting of a USB2000
11 miniature diode-array spectrometer with a 0.4 mm diameter fore-optic assembly attached to the
12 fibre tip (Ocean Optics, Dunedin, FL USA). With the aperture located 9 mm away from fiber tip,
13 the field of view was controlled by a cone angle of 2.5 degrees. The field of view (FOV) of the plot
14 canopy was therefore a 4 cm diameter circle at a fore-optic height of 1 m above the crop canopy.
15
16
17
18
19
20
21
22

23 The USB2000 miniature diode-array spectrometer is equipped with a 600 line-diffraction
24 grating blazed at 500 nm and a 200 µm input slit, giving the spectrometer a useable spectral range
25 of 400 - 900 nm and a spectral resolution of 1.5 nm. The diode-array spectrometer was connected to
26 an IPAQ Personal Digital Assistant (PDA) running PalmSpec Software (Ocean Optics, Dunedin,
27 FL USA). The spectrometer integration time was set to 5 milliseconds.
28
29
30
31
32
33
34
35

36 Radiance data were converted to reflectance values (0-1) by normalizing the collected spectra
37 against that produced by a >98% reflectance, Lambertian reflectance standard (30 mm diameter
38 Zenith™ disk, Newport Corporation, USA) presented in the same way as the crop canopy to the
39 reflectance probe.
40
41
42
43
44
45

46 Two measurements were recorded from each of the 40 experimental plots at GS 47 (booting
47 stage) and again at GS 75 (grain development stage). Visual measurements of the level of stripe rust
48 infection (ACRL scale) and N deficiency were carried out for each plot on the same day.
49
50
51
52
53
54
55
56
57
58
59
60
61
62
63
64
65

Results

Nitrogen – stripe rust interaction

1
2 Increasing rates of N application at sowing resulted in increased severity of stripe rust infection
3
4 in H45 for both with (+) and without (-) fungicide treatments (Fig. 2). However, this trend was
5
6 found to be statistically significant for the without (-) fungicide treatment only.
7
8

9
10 [Fig. 2 here]
11
12
13

Plant response to N status and stripe rust severity

14
15 Average spectral reflectance curves (400 – 900 nm; visible and NIR) were derived for each of
16
17 these classes for both N deficiency and stripe rust severity at GS 75 (Fig. 3).
18
19

20
21 A comparative analysis of the spectral signatures demonstrated that both high N deficiency and
22
23 high levels of stripe rust infection generally decreased reflectance in the red wavelength region of
24
25 the spectrum (~600-700 nm) (Fig. 3). However, the reflectance in the NIR region (>705 nm)
26
27 responded differently for high stripe rust infection compared to high N deficiency. Plants with high
28
29 levels of rust infection showed an increase in the NIR reflectance whereas high levels of N
30
31 deficiency reduced NIR reflectance.
32
33

34
35 [Fig. 3 here]
36
37

38 Percentage of reflectance for each 10 nm-narrow waveband regions across the entire visible-NIR
39
40 spectrum (400-1000 nm) was correlated with rust infection and N deficiency scores at GS 75 (Fig.
41
42 **4**). All the correlation coefficients between narrow band reflectance in the red wavelength region
43
44 and rust infection scores were significant ($p < 0.05$ or $p < 0.01$), however, reflectance in the NIR
45
46 region (750-920 nm) was significantly correlated with N deficiency scores ($p < 0.01$).
47
48

49
50 [Fig. 4 here]
51
52

53 The results of correlating the eleven VIs (Table 1) with the stripe rust and N levels at GS 47 are
54
55 summarised in Fig. 5. Some VIs had highly contrasting responses for increasing severity of stripe
56
57 rust infection and N deficiency. At GS 47, PhRI and ARI had the highest correlation with stripe rust
58
59 severity (significant at $P < 0.01$). The correlation of PRI with rust severity was also significant ($P <$
60
61 0.05). However, correlations of these three VIs with N deficiency were not significant.
62
63
64
65

[Fig. 5 here]

1
2 Conversely, LCCI and NDVI showed a highly significant ($P < 0.01$) negative correlation with N
3 deficiency. Other VIs such as NVI, TCARI, PSRI and SIPI were also found to be significantly ($P <$
4 0.05) correlated with N deficiency. Among these VIs that had a correlation with N deficiency, only
5
6 NVI also had a significant correlation with the severity of stripe rust infection.
7
8
9

10
11 The pattern of response of these VIs at GS 75 was almost similar to the GS 47 assessments with
12 a difference mainly in the magnitude of the relationship between VIs and crop condition (Fig. 6). At
13 both growth stages, PhRI, ARI and PRI had the highest correlation with stripe rust severity whereas
14 LCCI and NDVI had the highest correlations with N deficiency levels.
15
16
17
18
19
20

[Fig. 6 here]

21
22 Scatter plots of the indices that provided the strongest levels of correlation; PhRI for stripe rust
23 severity and LCCI for N deficiency are depicted in **Fig. 7**. PhRI, the most effective index for rust
24 discrimination, explained 68% of the variation in stripe rust severity. The coefficient of
25 determination using LCCI for N deficiency had a regression function that was slightly lower
26 explaining 56% of the variation (Fig. 6).
27
28
29
30
31
32
33
34
35

[Fig. 7 here]

36 37 38 39 ***Discriminating N status and stripe rust severity***

40
41 Based on the visual ratings of rust severity and N deficiency all the 40 plots were classified into
42 low, medium and high classes. Both these stress conditions were lower at GS 47 than at GS 75 with
43 no high level of disease severity or nutrient deficiency observed at the earlier assessment timing.
44
45 Further, rust severity and N deficiency were predicted using PhRI and LCCI, respectively, and
46 based on the predicted scores plots were classified into low, medium and high classes.
47
48
49
50
51
52
53

54
55 The plot-by-plot performance of the combined indices (PhRI and LCCI) for predicting stripe
56 rust severity and N deficiency is presented in a two-dimensional bubble graph (Fig 8). The level of
57 each predicted parameter (low, medium or high) was compared with the actual level. The x-axis
58 maps the outcome of the N deficiency prediction in terms of whether the predicted value is lower,
59
60
61
62
63
64
65

1
2
3
4
5
6
7
8
9
10
11
12
13
14
15
16
17
18
19
20
21
22
23
24
25
26
27
28
29
30
31
32
33
34
35
36
37
38
39
40
41
42
43
44
45
46
47
48
49
50
51
52
53
54
55
56
57
58
59
60
61
62
63
64
65

equal to or higher than the actual value. For example, if the N deficiency was predicted to be ‘low’, but the actual value was ‘high’ then it would be given a outcome of ‘-2’, i.e. two degrees of under-estimation. Similarly, if the predicted value was for ‘high’ when in fact the actual value was ‘medium’, then it would receive a value of ‘+1’, i.e. one degree of over-estimation. The same applies for the severity of stripe rust infection, this time allocated along the y-axis. The size of the bubbles in the plot is an indication of the percent of the 40 plots that fit within each category (percent values also numerically indicated).

[Fig 8 here]

In 82.5% of the plots, the combination of the two indices correctly classified both the N deficiency and stripe rust severity into low and medium category levels at GS 47, whereas accuracy was 55% at GS 75 where the severity of both stripe rust infection and N deficiency were much higher. In misclassified plots at GS 75, an over-estimation of N deficiency was more than likely accompanied by an under-estimation of the stripe rust infection level and vice-versa. In 92.5% of cases the two indices predicted both the level of stripe rust infection and N deficiency within one category level. This larger level of misclassification only occurred when predicting levels of stripe rust severity with one of the 40 plots (2.5%) being predicted as having high disease severity but visual assessments were actually low. Conversely, two plots (5%) were predicted by PhRI to have low levels of stripe rust severity but the actual visual rating was high. Interestingly, in all three of these plots LCCI correctly predicted the level of N deficiency.

Discussion

Consistent with previous studies (Ash and Brown 1991; Devadas et al. 2014), increased rates of N application increased the severity of stripe rust in wheat during grain fill. Analysis of the hyperspectral indices at crop growth stages GS 47 and GS 75 point to the contrasting response of different VIs to changes in stripe rust infection or N deficiency (**Fig. 5** and **Fig. 6**). Indices which were highly correlated with one of these parameters were found to be relatively insensitive to the

other. This indicates the possibility of using such indices in combination for discriminating the actual levels of stripe rust from N deficiency.

In a previous laboratory study (Devadas et al. 2009), the vegetation index ARI, which measures non-chlorophyll pigment concentration, was found to be most reliable in discriminating healthy leaves from those infected with stripe, stem or leaf rust. In this study, ARI was strongly correlated with stripe rust severity in the field, but less so than PhRI. In single leaf tests (Devadas et al. 2009) PhRI discriminated stripe rust infected leaves from healthy leaves, but not from those infected by stem rust or leaf rust. While the results of the current study suggests PhRI is the most effective index for determining the severity of stripe rust in the field, this is likely to be specific to this type of rust and it is unlikely to differentiate stripe rust from leaf and stem rust of wheat.

Although single leaf analysis (Devadas et al. 2009) indicated that indices like LCCI, NDVI, NPCI, NRI, PSRI and SIPI could be useful in discriminating stripe rust infected plants from healthy plants, correlation analysis of canopy data demonstrated that these indices were relatively ineffective in quantifying the changes due to stripe rust infection in the field. Higher stripe rust severity can be associated with plants having higher N availability and canopy density (Ash and Brown 1991; Danial and Parlevliet 1995). Therefore the retention of higher canopy densities to some extent would have created a higher NIR reflectance, which is a component of most of the indices used in this study.

Canopy hyperspectral data analysis in this study confirmed that PRI, PhRI and ARI were effective in discriminating different levels of stripe rust infection consistently. This is supported by previous studies where indices, PRI (Penuelas et al. 1995a; Trotter et al. 2002; Huang et al. 2007), PhRI (Gamon et al. 1992; Penuelas et al. 1994) and ARI (Gitelson et al. 2001) were found to be very effective for detecting changes in xanthophylls and carotenoid pigments and plant stress which are affected by stripe rust infection.

This study also consistently demonstrated that LCCI, NDVI, NVI and SIPI, which captured the changes in reflectance in the NIR region ($\approx 705-750$ nm), were the best indicators of N deficiency. These observations are in agreement with studies by Diker & Bausch (2003) and Gitelson &

Merzlyak (1994b) which investigated the potential of LCCI and NRI, respectively, for monitoring plant chlorophyll content and N nutrition.

1
2 These observations were well supported by the correlation analysis of narrow band reflectance
3 values with rust infection and N deficiency scores (**Fig. 4**). Rust infection was found to be
4 significantly correlated to reflectance in the mid-green to red wavelength regions and the most
5 effective indices in detecting rust infection (PhRI, PRI and ARI) mainly utilised reflectance in these
6 wavelength region. This analysis also indicated that reflectance in the NIR region were the most
7 useful in quantifying N deficiency and all the indices identified as the best indicators of N
8 deficiency (LCCI, NDVI, NVI and SIPI) incorporated the narrow band reflectance in the NIR
9 region.
10
11

12
13
14
15
16
17
18
19
20
21 The two indices with the highest correlation with either the level of N deficiency or stripe rust
22 severity had opposing responses in this study. Clearly N deficiency drove the LCCI up while stripe
23 rust infection drove the PhRI downwards. Never did the combined use of the two indices over- or
24 underestimate both parameters for any given plot. In 17.5% of the plots, there was a tendency to
25 underestimate the level of stripe rust infection even though the N deficiency level was correctly
26 predicted. However, in only 5% of cases was this under estimation in stripe severity greater than
27 one category (i.e. predicted low severity and visually assessed as high). The contrasting responses
28 of the PhRI and LCCI to the level of stripe rust infection and N deficiency, respectively, and the
29 relative insensitivity of these indices to other parameters makes their use in combination suitable for
30 quantifying levels of stripe rust infection and N deficiency in wheat crops.
31
32
33
34
35
36
37
38
39
40
41
42
43
44
45

46 Hyperspectral imaging techniques have been effectively utilized in other studies for the
47 detection of plant diseases, nutritional deficiency or physiological changes in pigmentation.
48 Accuracies of the assessment of these physiological changes were demonstrated to be high when
49 these conditions were analysed vis-à-vis a healthy plant canopy. However, under field conditions,
50 the interaction of plant nutrition and pest/disease infestation and consequent changes in plant
51 physiological and bio-chemical conditions are complex and difficult to quantify. This is further
52 complicated by the differences in plant phenotypic characteristics and ecosystem interactions.
53
54
55
56
57
58
59
60
61
62
63
64
65

1
2
3
4
5
6
7
8
9
10
11
12
13
14
15
16
17
18
19
20
21
22
23
24
25
26
27
28
29
30
31
32
33
34
35
36
37
38
39
40
41
42
43
44
45
46
47
48
49
50
51
52
53
54
55
56
57
58
59
60
61
62
63
64
65

Considering these issues, this study attempted to conduct a field experiment where interactions between stripe rust infection and N nutrition would be visible and there by quantified using both traditional and advanced imaging technologies. Remote sensing of plant canopy using hyperspectral data was found to be such a technology by which these complex interactions could be quantified successfully under field conditions. Visual rating of disease severity to determine resistance levels is quite subjective with potential assessor variation and often requires specialised training to minimise assessment error (Bock et al. 2010). Use of an independent hyperspectral technique by pathologists would minimise operator variation and assessment error with requirement for less specialised training. Wheat breeding programs could also potentially use these rapid and objective hyperspectral measures to phenotype stripe rust resistance levels in large scale replicated field evaluation plots with the ability to reliably discriminate infection levels from N deficiency.

Acknowledgments

The authors gratefully acknowledge the receipt of Postgraduate Funding from the University of New England (UNE) and Cooperative Research Centre for Spatial Information (CRCSI), Australia. The CRCSI was established and supported under the Australian Governments Cooperative Research Centres Programme. Authors are also thankful to the NSW Department of Primary Industries for the establishment of experimental plots at the Breeza research station in NSW.

References

- Aparicio, N., Villegas, D., & Casadesus, J. (2000). Spectral vegetation indices as non-destructive tools for determining durum wheat yield. *Agronomy Journal*, 92, 83-91.
- Ash, G. J., & Brown, J. F. (1991). Effect of nitrogen nutrition of the host on the epidemiology of *Puccinia striiformis* f.sp. *tritici* and crop yield in wheat. *Australian Plant Pathology*, 20(3), 108-114.
- Aspinall, R. J., Andrew Marcus, W., & Boardman, J. W. (2002). Considerations in collecting, processing, and analysing high spatial resolution hyperspectral data for environmental investigations. *Journal of Geographic Systems*, 4, 15-29.
- Blackburn, G. A. (1998). Spectral indices for estimating photosynthetic pigment concentrations: a test using senescent tree leaves *International Journal of Remote Sensing*, 19(4), 657-675.
- Bravo, C., Moshou, D., West, J., McCartney, A., & Ramon, H. (2003). Early Disease Detection in Wheat Fields using Spectral Reflectance. *Biosystems Engineering*, 84(2), 137-145.

- 1 Bryson, R. J., Paveley, N. D., Clark, W. S., Sylvester-Bradley, R., & Scott, R. K. (1997). Use of in-
2 field measurements of green leaf area and incident radiation to estimate the effects of yellow
3 rust epidemics on the yield of winter wheat. *European Journal of Agronomy*, 7(1-3), 53-62.
- 4 Campbell, J. B. (1996). *Introduction to remote sensing* (Second ed.): The Guilford Press, New
5 York.
- 6 Caviglia, O. P., & Sadras, V. O. (2001). Effect of nitrogen supply on crop conductance, water- and
7 radiation-use efficiency of wheat. *Field Crops Research*, 69(3), 259-266.
- 8 Danial, D. L., & Parlevliet, J., E (1995). Effects of nitrogen fertilization on disease severity and
9 infection type of yellow rust on wheat genotypes varying in quantitative resistance. *Journal
10 of Phytopathology*, 143, 679-681.
- 11 Devadas, R., Lamb, D. W., Simpfendorfer, S., & Backhouse, D. (2009). Evaluating ten spectral
12 vegetation indices for identifying rust infection in individual wheat leaves *Precision
13 Agriculture*, 10, 459-470, doi:10.1007/s11119-008-9100-2.
- 14 Devadas, R., Simpfendorfer, S., Backhouse, D., & Lamb, D. W. (2014). Effect of stripe rust on the
15 yield response of wheat to nitrogen. *The Crop Journal*, 2(4), 201-206,
16 doi:<http://dx.doi.org/10.1016/j.cj.2014.05.002>.
- 17 Diker, K., & Bausch, W. C. (2003). Potential Use of Nitrogen Reflectance Index to estimate Plant
18 Parameters and Yield of Maize. *Biosystems Engineering*, 85(4), 437-447.
- 19 Filella, I., Serrano, L., Serra, J., and Penuelas, J. (1995). Evaluating wheat nitrogen status with
20 canopy reflectance indices and discriminant analysis. *Crop Science*, 35, 1400-1405.
- 21 Gamon, J. A., Penuelas, J., & Field, C. B. (1992). A narrow-waveband spectral index that tracks
22 diurnal changes in photosynthetic efficiency. *Remote Sensing of Environment*, 41(1), 35-44.
- 23 Gao, J. (1999). A comparative study on spatial and spectral resolutions of satellite data in mapping
24 mangrove forests. *International journal of remote sensing*, 20(14), 2823-2833.
- 25 Gitelson, A., & Merzlyak, M. N. (1994a). Quantitative estimation of chlorophyll-a using reflectance
26 spectra: Experiments with autumn chestnut and maple leaves. *Journal of Photochemistry
27 and Photobiology B: Biology*, 22(3), 247-252.
- 28 Gitelson, A., & Merzlyak, M. N. (1994b). Spectral reflectance changes associate with autumn
29 senescence of *Aesculus hippocastanum* L., and *Acer platanoides* L. leaves. Spectral features
30 and relation to chlorophyll estimation. *Journal of Plant Physiology*, 143, 286-292.
- 31 Gitelson, A. A., Merzlyak, M. N., & Chivkunova, O. B. (2001). Optical properties and
32 nondestructive estimation of anthocyanin content in plant leaves. *Photochemistry and
33 Photobiology*, 74(1), 38-45.
- 34 Gooding, M. J., & Davies, W. P. (1997). *Wheat production and utilization - systems, quality and the
35 environment*: CAB International, New York, USA.
- 36 Gupta, R. K., Vijayan, D., & Prasad, T. S. (2001). New hyperspectral vegetation characterization
37 parameters. *Advances in Space Research*, 28(1), 201-206.
- 38 Haboudane, D., Miller, J. R., Tremblay, N., Zarco-Tejada, P. J., & Dextraze, L. (2002). Integrated
39 narrow-band vegetation indices for prediction of crop chlorophyll content for application to
40 precision agriculture. *Remote Sensing of Environment*, 81(2-3), 416-426.
- 41 Hansen, P. M., & Schjoerring, J. K. (2003). Reflectance measurement of canopy biomass and
42 nitrogen status in wheat crops using normalized difference vegetation indices and partial
43 least squares regression. *Remote Sensing of Environment*, 86(4), 542-553.
- 44 Hatfield, P. L., and Pinter, Jr, P. J. (1993). Remote sensing for crop protection. *Crop Protection*,
45 12(6), 403-413.
- 46 Huang, W., Lamb, D. W., Niu, Z., Zhang, Y., Liu, L., & Wang, J. (2007). Identification of yellow
47 rust in wheat using in-situ spectral reflectance measurements and airborne hyperspectral
48 imaging. *Precision Agriculture*, 8, 187-197, doi:DOI 10.1007/s11119-007-9038-9.
- 49 Jensen, B., & Munk, L. (1997). Nitrogen induced changes in colony density and spore production of
50 *Erysiphe graminis* f.sp. *hordei* on seedlings of six spring barley cultivars. *Plant Pathology*
51 46, 191-202.
- 52 McRae, F. J., McCaffery, D. W., & Matthews, P. W. (2008). Winter Crop Variety Sowing Guide.
53 <http://www.sfs.org.au/LiteratureRetrieve.aspx?ID=97401>. Accessed 26-11-2014.

- Merzlyak, M. N., Gitelson, A. A., Chivkunova, O. B., & Rakitin, V. Y. (1999). Non-destructive optical detection of pigment changes during leaf senescence and fruit ripening. *Physiologia Plantarum*, 106, 135- 141.
- 1 Moshou, D., Bravo, C., Oberti, R., West, J., Bodria, L., McCartney, A., et al. (2005). Plant disease
2 detection based on data fusion of hyper-spectral and multi-spectral fluorescence imaging
3 using Kohonen maps. *Real-Time Imaging*, 11(2), 75-83.
- 4 Muurinen, S., & Peltonen-Sainio, P. (2006). Radiation-use efficiency of modern and old spring
5 cereal cultivars and its response to nitrogen in northern growing conditions. *Field Crops
6 Research*, 96, 363-373.
- 7
8 Nicolas, H. (2004). Using remote sensing to determine of the date of a fungicide application on
9 winter wheat. *Crop Protection*, 23(9), 853-863.
- 10 Penuelas, J., Baret, F., & Filella, I. (1995a). Semi-empirical indices to assess
11 carotenoids/chlorophyll a ratio from leaf spectral reflectance. *Photosynthetica*, 31(221- 230).
- 12 Penuelas, J., Filella, I., & Gamon, J. A. (1995b). Assessment of photosynthetic radiation-use
13 efficiency with spectral reflectance. *New Phytologist*, 131, 291-296.
- 14 Penuelas, J., Gamon, J. A., Fredeen, A. L., Merino, J., & Field, C. B. (1994). Reflectance indices
15 associated with physiological changes in nitrogen- and water-limited sunflower leaves.
16 *Remote Sensing of Environment*, 48(2), 135-146.
- 17
18 Qin, Z., & Zhang, M. (2005). Detection of rice sheath blight for in-season disease management
19 using multispectral remote sensing. *International Journal of Applied Earth Observation and
20 Geoinformation*, 7(2), 115-128.
- 21
22 Snowball, K., & Robson, A. D. (1991). Nutrient Deficiencies and Toxicities in Wheat: A Guide for
23 Field Identification. Mexico, D.F.: CIMMYT.
- 24
25 Spectrum (2009). SPAD 502 plus Chrophyll Meter - Product Manual.
26 http://www.specmeters.com/assets/1/22/2900P_SPAD_502.pdf. Accessed 7-1-2015.
- 27
28 Tarpley, L., Reddy, K., & Sassenrath-Cole, F. (2000). Reflectance indices with precision and
29 accuracy in predicting cotton leaf nitrogen concentration. *Crop Science*, 40, 1814-1819.
- 30 Trotter, G. M., Whitehead, D., & Pinkney, E. J. (2002). The photochemical reflectance index as a
31 measure of photosynthetic light use efficiency for plants of varying foliar nitrogen contents.
32 *International Journal of Remote Sensing*, 23(6), 1207-1212.
- 33
34 Tucker, C. J. (1979). Red and photographic infrared linear combination for monitoring vegetation.
35 *Remote Sensing of Environment*, 8, 127-150.
- 36 Tucker, C. J., Holben, B. N., Elgin Jr, J. H., & McMurtrey Iii, J. E. (1981). Remote sensing of total
37 dry-matter accumulation in winter wheat. *Remote Sensing of Environment*, 11(0), 171-189,
38 doi:[http://dx.doi.org/10.1016/0034-4257\(81\)90018-3](http://dx.doi.org/10.1016/0034-4257(81)90018-3).
- 39
40 Wellings, C., & Bariana, H. (2004). Assessment scale for recording stripe rust responses in field
41 trials. http://www.grdc.com.au/uploads/documents/stripe_rust2.pdf. Accessed 26-11-2014.
- 42
43 Young, A., & Britton, G. (1990). Carotenoids and stress. In R. G. Alscher, & J. R. Cumming (Eds.),
44 *Stress Responses in Plants: Adaptation and Acclimation Mechanisms* (pp. 87-112). New
45 York: Wiley.
- 46
47 Zhao, D. H., Li, J. L., & Qi, J. G. (2005a). Identification of red and NIR spectral regions and
48 vegetative indices for discrimination of cotton nitrogen stress and growth stage. *Computers
49 and Electronics in Agriculture*, 48(2), 155-169.
- 50
51 Zhao, M., Heinsch, F. A., Nemani, R. R., & Running, S. W. (2005b). Improvements of the MODIS
52 terrestrial gross and net primary production global data set. *Remote Sensing of Environment*,
53 95(2), 164-176.
- 54
55
56
57
58
59
60
61
62
63
64
65

Table 1 Hyperspectral indices used in this study for the assessment of plant pigments and vegetation condition.

Index Name	Formula	Association with relevant plant pigment	Reference example
Leaf and Canopy	$LCCI = \left(\frac{R_{750} - R_{705}}{R_{750} + R_{705}} \right)$	Indicator of chlorophyll content and hence early stages of leaf senescence as R_{705} is maximally and R_{750} is minimally sensitive to chlorophyll	(Gitelson and Merzlyak 1994a, 1994b)
Normalised	$NDVI = \left(\frac{NIR - R}{NIR + R} \right)$	NIR and Red are broad reflectance bands 775-825 nm (NIR) and 650-700 nm (R) that include most key pigments. NDVI increases with leaf area index (LAI) and photosynthetically active radiation (PAR) or biomass (PAB).	(Campbell 1996; Tucker 1979; Tucker et al. 1981)
Difference			
Vegetation Index			
New Vegetation Index	$NVI = \left(\frac{R_{777} - R_{747}}{R_{673}} \right)$	Sensitive to chlorophyll <i>a</i> and <i>b</i>	(Gupta et al. 2001)
The Physiological			
Reflectance Index	$PhRI = \left(\frac{R_{550} - R_{531}}{R_{550} + R_{531}} \right)$	Follows diurnal changes in the xanthophyll pigments and photosynthetic rates.	(Gamon et al. 1992; Penuelas et al. 1994)
Nitrogen			
Reflectance Index	$NRI = \left(\frac{R_{570} - R_{670}}{R_{570} + R_{670}} \right)$	Similar to NDVI above- but strictly relevant to nitrogen and hence chlorophyll- <i>a</i> .	(Aparicio et al. 2000; Diker and Bausch 2003; Fiella 1995; Hansen and Schjoerring 2003; Tarpley et al. 2000; Zhao et al. 2005a; Zhao et al. 2005b)
Normalised Pigment			
Chlorophyll Ratio	$NPCI = \left(\frac{R_{680} - R_{430}}{R_{680} + R_{430}} \right)$	Ratio of carotenoids relative to chlorophyll due to nitrogen stress and NPCI varies with the ratio of total pigments to chlorophyll. Used to evaluate the proportion of total photosynthetic pigments to chlorophyll.	(Young and Britton 1990; Penuelas et al. 1994)
Index			
Anthocyanin			
Reflectance Index	$ARI = \left(\frac{1}{R_{550}} \right) - \left(\frac{1}{R_{700}} \right)$	Anthocyanin accumulation is induced by strong light, UV-B irradiation, low temperature, drought, wounding, bacterial and fungal infections, nitrogen and phosphorus deficiencies. ARI proposed for the estimation for accumulation of anthocyanin in intact senescing and stressed leaves	(Gitelson et al. 2001)

1			
2			
3			
4	Photochemical		
5	$PRI = \left(\frac{R_{570} - R_{531}}{R_{570} + R_{531}} \right)$	R_{531} associated with state of the xanthophyll cycle and as xanthophyll pigments fulfill a photoprotective role, and key to light use efficiency (LUE). High levels of xanthophyll activity are thus associated with high stress (low LUE).	(Trotter et al. 2002; Pennuelas et al. 1994; Pennuelas et al. 1995b)
6	reflectance index		
7			
8			
9			
10			
11	The Structure-		
12			
13	In sensitive Pigment		
14	$SIP1 = \left(\frac{R_{800} - R_{445}}{R_{800} + R_{680}} \right)$	Used to estimate the ratio of carotenoids to chlorophyll- <i>a</i> .	(Pennuelas et al. 1995a; Blackburn 1998)
15	Index		
16			
17	Plant Senescence		
18			
19	Reflectance Index		
20			
21			
22	The transformed		
23	chlorophyll		
24	$TCARI = 3 \left[(R_{700} - R_{600}) - 0.2 (R_{700} - R_{550}) \left(\frac{R_{700}}{R_{670}} \right) \right]$	Highly sensitive to chlorophyll pigments	(Haboudane et al. 2002)
25	Absorption and		
26			
27	Reflectance Index		
28			
29			
30			
31			
32			
33			
34			
35			
36			
37			
38			
39			
40			
41			
42			
43			
44			
45			
46			
47			
48			
49			

1
2
3
4
5
6
7
8
9
10
11
12
13
14
15
16
17
18
19
20
21
22
23
24
25
26
27
28
29
30
31
32
33
34
35
36
37
38
39
40
41
42
43
44
45
46
47
48
49
50
51
52
53
54
55
56
57
58
59
60
61
62
63
64
65

Table 2 Number of observations recorded for each class of rust infection and N deficiency

Clas	GS 47		GS 75	
	Rust	N	Rust	N
Low	36	34	20	24
Med	4	6	8	8
High	0	0	12	8

1
2
3
4
5
6
7
8
9
10
11
12
13
14
15
16
17
18
19
20
21
22
23
24
25
26
27
28
29
30
31
32
33
34
35
36
37
38
39
40
41
42
43
44
45
46
47
48
49
50
51
52
53
54
55
56
57
58
59
60
61
62
63
64
65

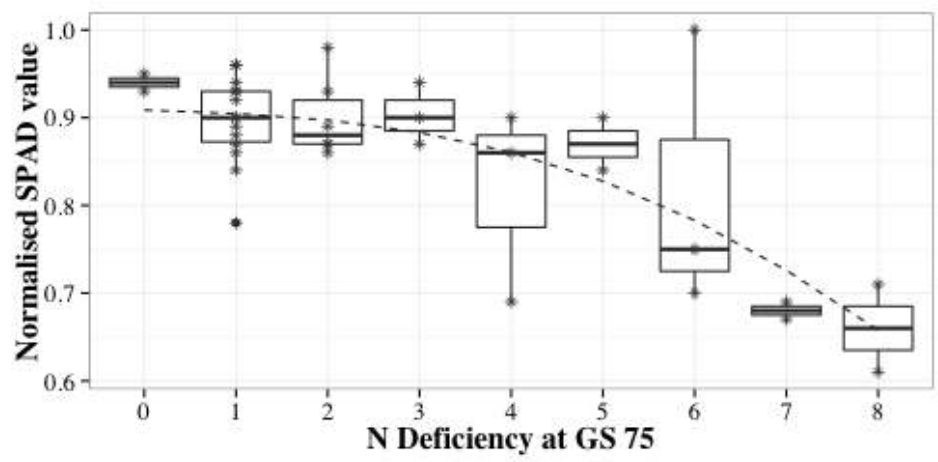


Fig 1. Comparison of visual scores of N deficiency and normalised SPAD value at GS 75

1
2
3
4
5
6
7
8
9
10
11
12
13
14
15
16
17
18
19
20
21
22
23
24
25
26
27
28
29
30
31
32
33
34
35
36
37
38
39
40
41
42
43
44
45
46
47
48
49
50
51
52
53
54
55
56
57
58
59
60
61
62
63
64
65

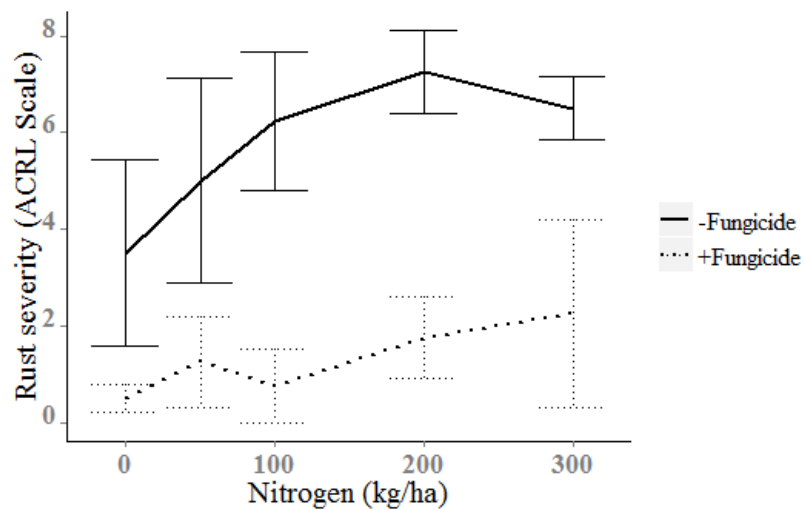


Fig. 2 Severity of stripe rust in H45 wheat during grain fill (GS 75) in 2007 at different nitrogen levels with (+) and without (-) fungicide treatment. Error bars show \pm standard errors (n = 4).

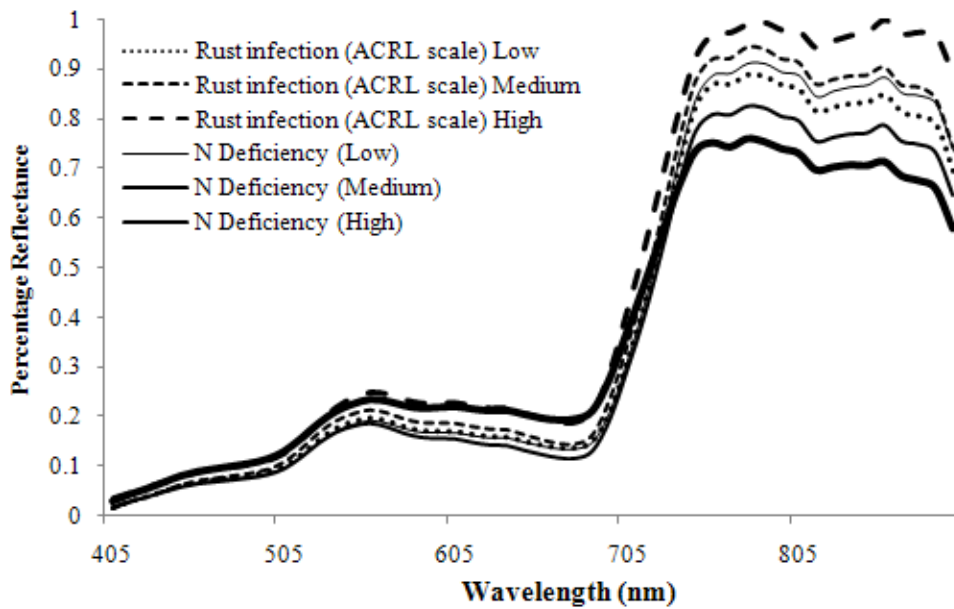


Fig. 3 Spectral signatures for different levels of stripe rust infection and N deficiency at GS 75 in the wheat variety H45 in 2007. These spectra represent average of spectral measurements of each category of rust infection and N deficiency as outlined in Table 2.

1
2
3
4
5
6
7
8
9
10
11
12
13
14
15
16
17
18
19
20
21
22
23
24
25
26
27
28
29
30
31
32
33
34
35
36
37
38
39
40
41
42
43
44
45
46
47
48
49
50
51
52
53
54
55
56
57
58
59
60
61
62
63
64
65

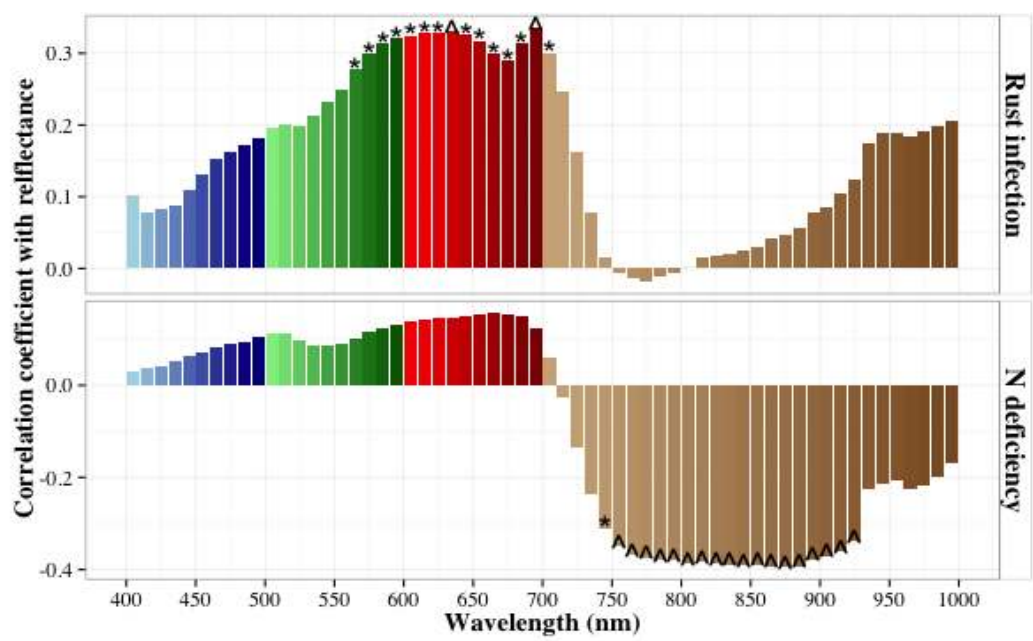


Fig. 4. Correlation coefficient of narrow waveband reflectance with rust infection and N deficiency at GS 75. Statistical significance of correlation coefficient is indicated with '*' for $p < 0.05$ and '^' for $p < 0.01$.

1
2
3
4
5
6
7
8
9
10
11
12
13
14
15
16
17
18
19
20
21
22
23
24
25
26
27
28
29
30
31
32
33
34
35
36
37
38
39
40
41
42
43
44
45
46
47
48
49
50
51
52
53
54
55
56
57
58
59
60
61
62
63
64
65

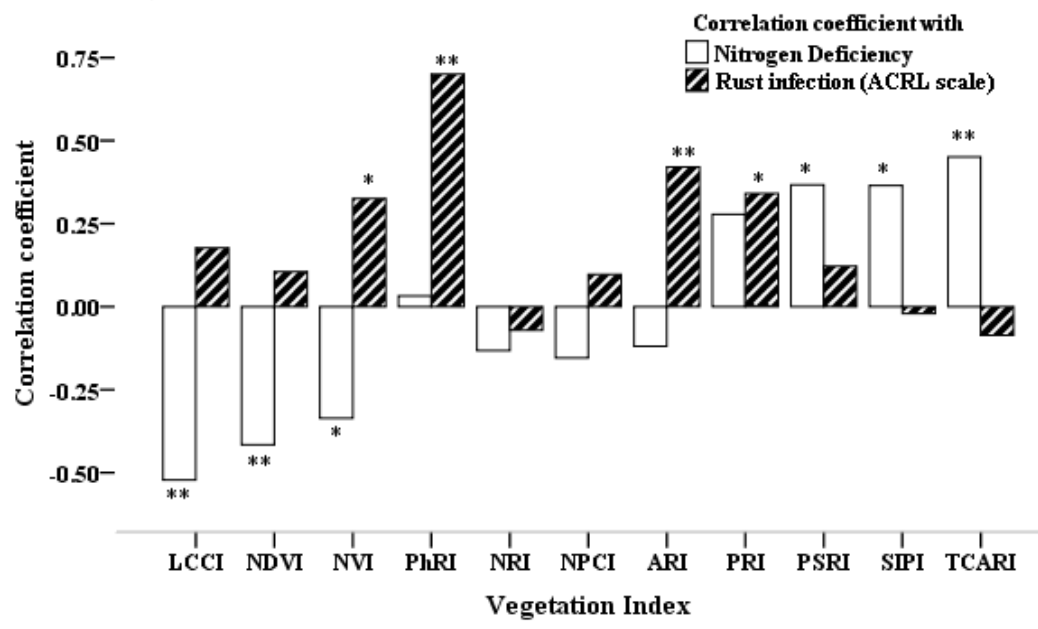


Fig. 5 Correlation of different VIs with stripe rust severity and the level of nitrogen deficiency at GS 47 in the wheat variety H45 in 2007.

*** indicates significance at 1% level and * at 5% level.*

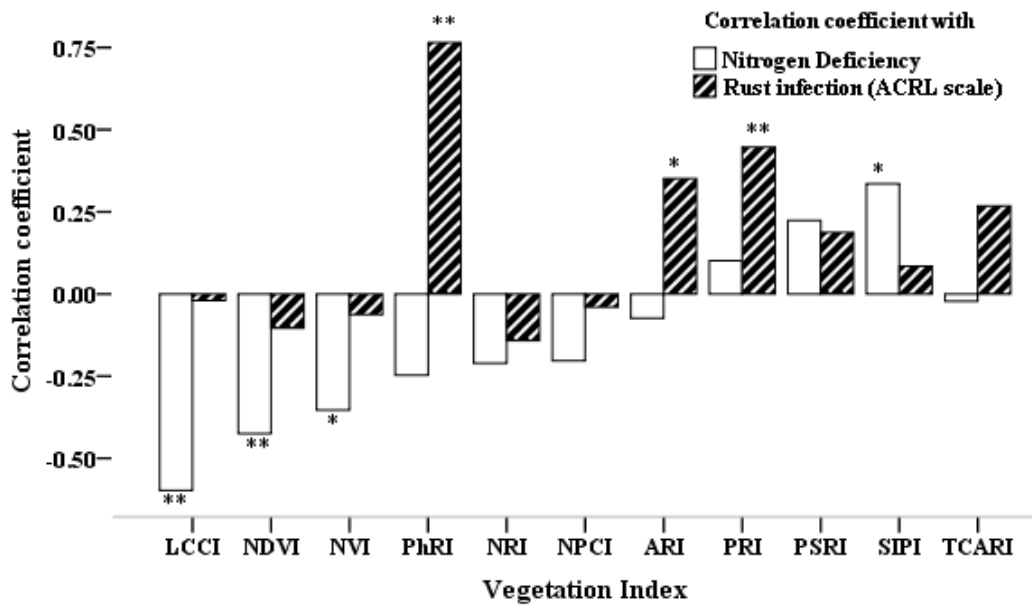
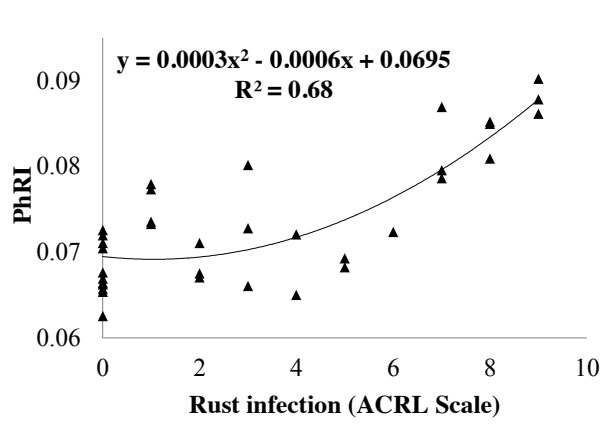


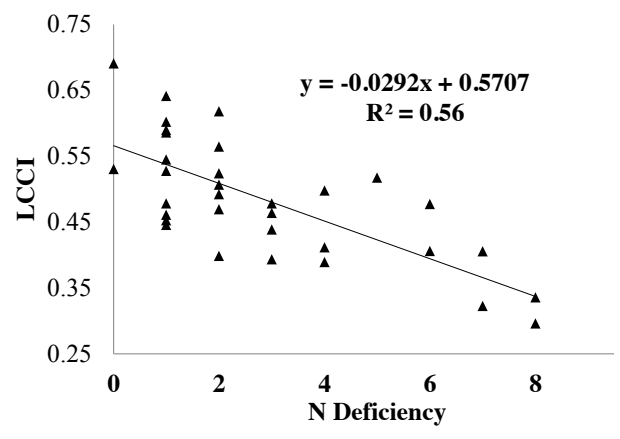
Fig. 6 Correlation of different VIs with stripe rust severity and the level of N deficiency at GS 75 in the wheat variety H45 in 2007.

** indicates significance at 1% level and * at 5% level.

1
2
3
4
5
6
7
8
9
10
11
12
13
14
15
16
17
18
19
20
21
22
23
24
25
26
27
28
29
30
31
32
33
34
35
36
37
38
39
40
41
42
43
44
45
46
47
48
49
50
51
52
53
54
55
56
57
58
59
60
61
62
63
64
65

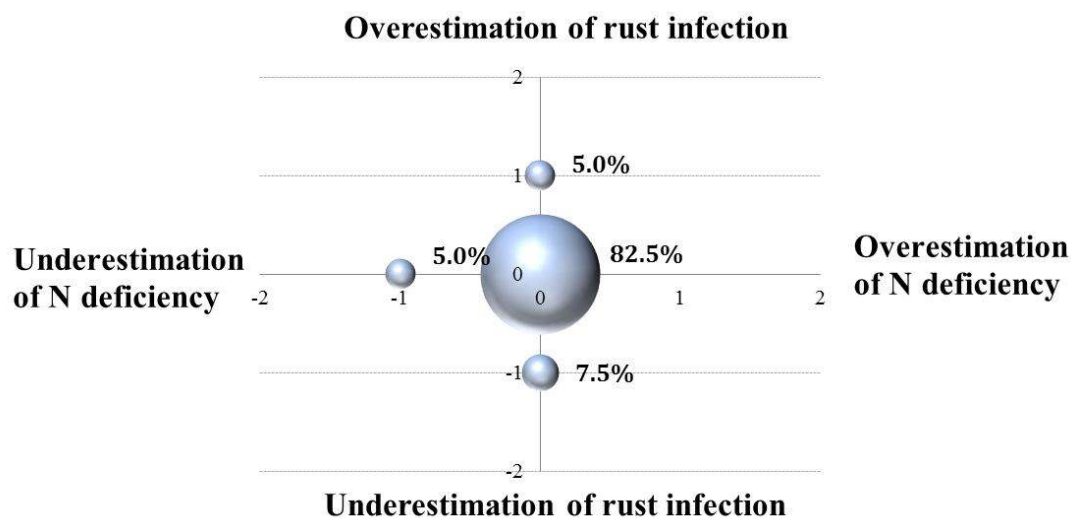


(a)

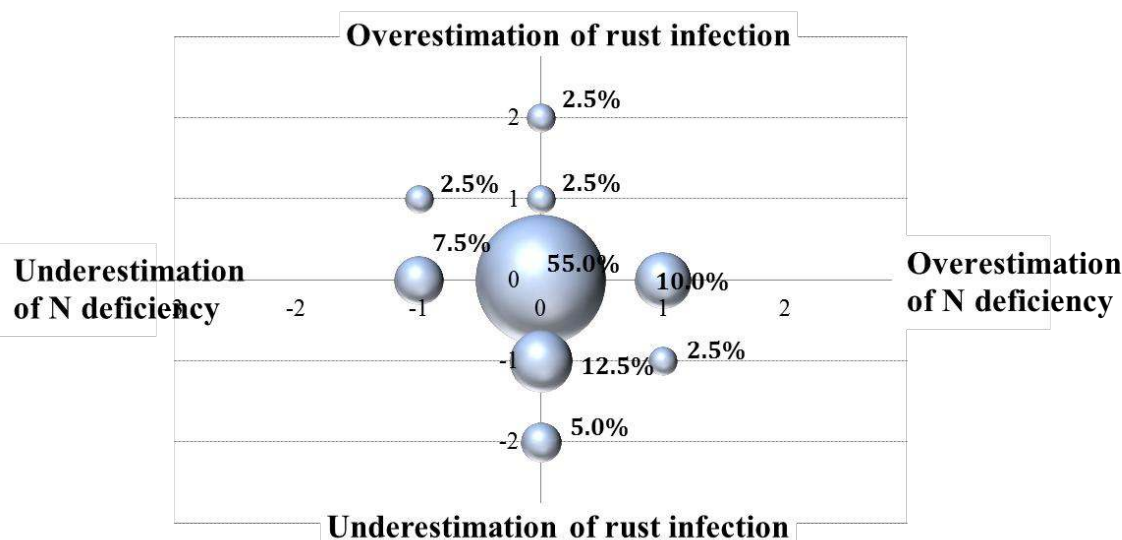


(b)

Fig. 7 Relationship between (a) level of stripe rust infection and PhRI and (b) N deficiency and LCCI at GS 75 in the wheat variety H45 in 2007.



a)



b)

Fig 8. Two-dimensional bubble graph mapping the combined performance of the PhRI for estimating stripe rust infection and the LCCI for estimating N deficiency at a) GS 47 and b) GS 75. The x and y-axes indicate the degree of over- or underestimation of each parameter; a unit of '±1' corresponding to the interval between a level of 'high' and 'medium', or 'medium' and 'low', and a value of '±2' indicates the difference between high and low.